Electrochemical and Spectroscopic Investigation of Bioactive Naphthoquinones

Erivaldo de Oliveira Costa,[1] María Teresa Molina,[2] Fabiane Caxico de Abreu,[1] Francisco de Assis dos Santos Silva,[1] Cicero de Oliveira Costa,[1] Waldomiro Pinho Jr.,[1] Iara B. Valentim,[1] Benjamín Aguilera–Venegas,[3] Fernanda Pérez-Cruz,[3] Ester Norambuena,[4] Claudio Olea-Azar,[3,] Marília O. F. Goulart[1,5,*]*

[1] Instituto de Química e Biotecnologia, Universidade Federal de Alagoas, Maceió, Alagoas, 57072-970, Brazil
[2] Instituto de Química Médica – Consejo Superior de Investigaciones Científicas (IQM-CSIC), Juan de la Cierva, 3, 28006-Madrid, Spain.
[3] Departamento de Química Inorgánica y Analítica, Facultad de Ciencias Químicas y Farmacéuticas, Universidad de Chile, Casilla 233, Santiago 1, Chile.
[4] Departamento de Química, Universidad Metropolitana de Ciencias de la Educación
[5] INCT - Bioanalítica
[*] E-mail: mariliaofg@gmail.com; colea@ciq.uchile.cl

The present work aims to investigate the electrochemical behavior of nine naphthoquinones, in aprotic and protic media. The reduction mechanism of the quinones in aprotic medium was proposed, with involvement of anion radical species, confirmed by performing *in-situ* Electrochemical-Electron Spin Resonance (E-ESR) experiments. Theoretical calculations using DFT method (U)B3LYP/6-31 were developed in order to rationalize the experimental hyperfine coupling constants. The results were in good agreement with the experimental data when solvent effects were included in the DFT models.

1. INTRODUCTION

Despite some intrinsic difficulties, electrochemical techniques have been extensively used to clarify drugs' mechanism of action, providing excellent insights into the mode of action of agents, and inspiring further drug design [1, 2]. The main contributions, which are in the field of cancer research, combine electrochemical and spectroscopic methods, in particular those used to analyze free radicals, (e.g. ESR) [3, 4]. These studies mainly focus on the activation of drugs by reduction or oxidation,

and/or their influence on redox homeostasis.-The versatility of electrochemical methodology allows the modelling of a multitude of biological milieus [1, 5]. The cyclic voltammetric technique, in aprotic medium, provides a very adequate procedure to evaluate the stability of electrogenerated radical anions, and together with spectroscopic methods, in particular those used to analyze free radicals, (e.g. ESR) give important information about radicals' formation [4]. In this medium, quinones and their corresponding anions are solvated far less efficiently than in water. Moreover, aprotic solvents mimic nonpolar environments of the cell where much of the biological electron transfer occurs [1, 5-11], which complements the results obtained during in vivo analysis. In protic medium, electrochemical studies model hydrophilic media [1, 5].

Some classes of bioactive compounds require bioreduction to exert their biological roles. In thermodynamic terms, if the reduction potential of an electroactive compound in buffered aqueous media (pH ~ 7) is more positive than -0.5 V *vs*. NHE, the enzymatic transfer of electrons is possible *in vivo*. A large number of physiologically active compounds display reduction potentials in the range of –0.5 V up to 0.0 *vs*. NHE [1, 5]. This range overlaps those of the biological reductants (around -0.4 V *vs*. NHE) and that of $O_2/O_2^{\bullet-}$, *ca.* –0.2 V *vs*. NHE. Among them, quinones still account for one of the largest families of electrochemical and biologically active compounds [1].

Naphthoquinones are one of the groups of secondary metabolites widespread in nature. They have many physiological roles. The interest of many investigators is due to their broad-range of biological activities [12-14]. The striking feature of quinone chemistry is the ease of reduction and therefore the ability to act as oxidizing or dehydrogenating agents, the driving force being the formation of a fully aromatic system. In general, two major mechanisms of quinone cytotoxicity have been proposed: stimulation of oxidative stress and alkylation of cellular nucleophiles, which encompass large range of biomolecules such as DNA and some enzymes. The knowledge and study of the electrochemical properties of these compounds, as well as, the analysis of its reduction products, either a semiquinone or a hydroquinone, are essential to their biological activity understanding, once it can mimic biological cycles of oxidation and reduction [1]. In the case of quinones which produce oxidative stress, the initiation of cell damage lies in the ability to form free-radical metabolites. The stability of these radical intermediates (formed through NADPH/NADP+ cycling), seems to determine both the type and degree of biological activity [15,16].

As such, the present work aims to investigate the electrochemical behavior of nine naphthoquinones (Figure 1), in aprotic and protic media. Those compounds were already assayed as larvicidal, against *Aedes aegypti*, as molluscicidal [14] and as cytotoxic against cancer cell lines [13]. Electrochemical-Electron Spin Resonance (E-ESR) experiments, together with theoretical calculations using DFT method (U)B3LYP/6-31 were developed in order to rationalize the electrochemical behavior in aprotic medium (DMSO + tetrabutyl ammonium perchlorate (TBAP) on hanging drop mercury electrode (HDME). Electrochemical data were obtained for some of the quinones, in protic media, using glassy carbon electrode (GCE).
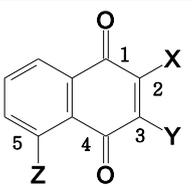
	X	Y	Z
Q1	H	H	OH
Q2	H	H	OAc
Q3	H	H	OMe
Q4	Br	H	OH
Q5	Br	H	OAc
Q6	Br	H	OMe
Q7	H	Br	OH
Q8	H	Br	OAc
Q9	H	Br	OMe

Figure 1. Chemical structures of juglone (Q1) and its derivatives (Q2 - Q9).

2. MATERIAL AND METHODS

2.1 Chemicals

All the juglone (Q1) derivatives Q2-Q9 (Figure 1) used in this study are known compounds and were prepared according to the methods described in the literature and reported in references 13 and 14. In summary, juglone (Q1) is a commercial material (Sigma-Aldrich, St. Louis, USA). Acetylation of juglone under standard conditions afforded juglone acetate (Q2). Compound Q3 was prepared by methylation of juglone (methyl iodide, silver (I) oxide) and compound Q4, prepared by hydrolysis of the corresponding acetate Q5. Methylation of Q4 led to the corresponding methyl ether Q6. The 3-bromojuglone derivatives (Q7-Q9) were prepared by selective bromination of juglone, which yielded Q7 as the major isomer. From Q7, either by standard acetylation or methylation, compounds Q8 or Q9, respectively, were obtained (Figure 1). All the physico-chemical (IR, MS, ^{1}H-NMR, ^{13}C-NMR) data are compatible with the chemical structures of the compounds [13, 14].

Acetic acid (CH$_3$COOH), sodium acetate (CH$_3$COONa), absolute ethanol (CH$_3$CH$_2$OH), sodium hydroxide (NaOH) and hydrochloric acid (HCl) were acquired from Merck, Rio de Janeiro, Brazil. Acetate and phosphate buffers and other solutions were prepared with water purified in a Milli-Q Millipore system and the pH values were determined with a Corning pH/Ion Analyzer 350 model.

2.2 Electrochemical experiments in aprotic medium

Cyclic voltammetry (CV) was carried out on a Metrohm 693 VA instrument with a 694 VA Stand convertor and a 693 VA Processor and a three-electrode cell under nitrogen atmosphere at room

temperature using DMSO (spectroscopic grade) + tetrabutyl ammonium perchlorate (TBAP) (0.1 mol L^{-1}), as supporting electrolyte. A hanging drop mercury electrode (HDME) was used as the working electrode, a platinum wire as the auxiliary electrode, and saturated calomel (SCE), as the reference electrode.

2.3 Electrochemical methods in protic medium

Electrochemical experiments, including cyclic voltammetry (CV) and differential pulse voltammetry (DPV), were performed using an Autolab (Echo-Chemie, Utrecht, Netherlands) PGSTAT 30. The working electrode was a BAS (Bioanalytical Systems, West Lafayette, IN, USA) GC electrode of 3 mm diameter, the counter electrode was a platinum coil, and the reference electrode was Ag|AgCl, Cl^- (0.1 mol L^{-1}), and all were contained in a one-compartment electrochemical cell of 10 mL capacity, using a volume of 5 mL. Stock solutions (1.0 mmol L^{-1}) of the quinones were prepared and kept protected against light, using ethanol/acetate buffer solution (20%, v/v). For DPV measurements, the pulse amplitude was 50 mV, the step potential was 10 mV and the scan rate was 0.005 Vs^{-1}. All experiments were performed at room temperature (25 $\pm$ 1°C).

2.4 Electron spin resonance spectroscopy

ESR spectra were recorded in the X band (9.85 GHz), using a Bruker ECS 106 spectrometer with a rectangular cavity and 50 kHz field modulation. The hyperfine splitting constants were estimated to be accurate within 0.05 G. The Q1-Q9 radicals were generated by electrolytic reduction *in situ* at room temperature under the same conditions as for the electrochemical case. ESR spectra of the anion radicals were obtained from the electrolysis solution. The ESR spectra were simulated using the program WINEPR Simphonia 1.25 version and ROKI package software [17].

2.5 Theoretical Calculations

The compounds Q1 - Q9 (Figure 1) were fully optimized to different level theory to reach the best degree of exactitude and precision in the calculations, in order to perform a fine-prediction of the hyperfine splitting pattern. For obtaining the best structure and finding the minimum energy structures with the highest abundant conformer population in the gas phase, a conformational search was performed using molecular mechanics methods (MMFF) as implemented in Spartan' 04 [18, 19]. Then, the best conformer was optimized with the AM1 semiempirical method [20], using Spartan. The last geometry optimization for each selected conformer was performed by means of density functional theory (DFT) as implemented in the GAUSSIAN' 03 package [21] since it is well known that computational models based on density functional theory (DFT) are particularly suitable for the analysis of magnetic properties for open-shell species [22]. The Q1-Q9 anion radicals structures were built using Becke's three parameter exact exchange functional (B3) [23] combined with gradient corrected correlation functional of Lee-Yang-Parr (LYP) [24] of DFT method (U)B3LYP/6-31G in

vacuum and also with the Conductor-like Polarizable Continuum Model (C-PCM), using DMSO as a solvent for testing the environment influence on the hyperfine splitting [25-27] in the single-point calculations. Single point calculations were performed using the basis sets of contracted Gaussian functions, namely 6-31+G (into the U-DFT model); all them upon the respective solvation model. All calculations were carried out under the unrestricted formalism; giving $<S^2>$ values lower than 0.7615, implicating a spin contamination less than of 2.0 percent.

3. RESULTS

3.1. Electrochemical studies in aprotic medium

Cyclic voltammograms, performed in DMSO + TBAP 0.1 mol L^{-1}, for the compounds without 5-OH group (Q-OR) (compounds Q2, Q3, Q5, Q6, Q8 and Q9, Figure 1) displayed two successive one-electron reduction processes, in a typical profile for quinones, in aprotic media (Figure 2). The width of the first cathodic wave at its half current intensity (W$_{1/2}$) has a relatively constant value of 60 mV.
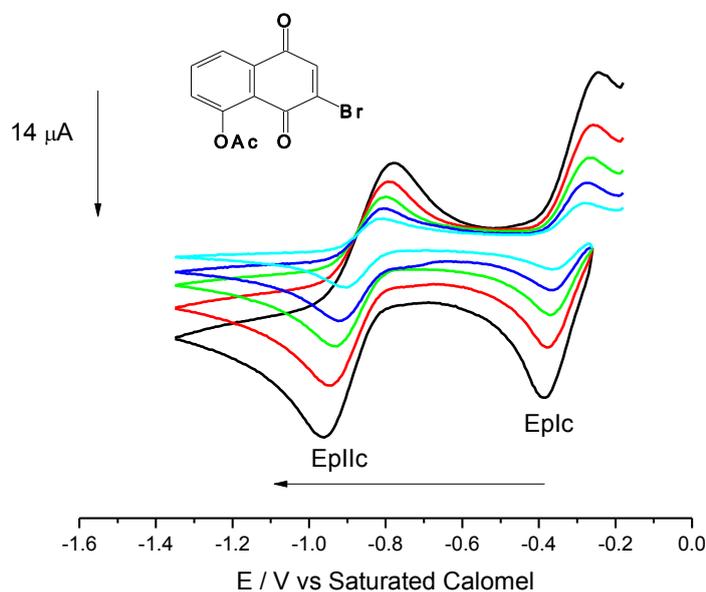
Figure 2. Cyclic voltammograms of Q8 (1 mM) in aprotic medium (DMSO + 0.1 M TBAP) and at different sweep rates (between 100 and 2000 mV s^{-1}).

The current intensity ratio Ip_a/Ip_c has a value close to unity. According to the standard reversibility criteria, this couple corresponds to a reversible diffusion-controlled monoelectronic transfer. It is related to the reduction of quinone to the semiquinone (Eq. 1), a stable anion radical at room temperature. The second couple is quasi-reversible over the whole range of scan rates used (100-2000 mV s^{-1}) (Figure 2) and is connected with the reduction of the semiquinone into the corresponding dianionic species (Eq. 2) (Table 1).

$$Q\text{-}OR + e \iff Q\text{-}OR^{\bullet} \qquad\qquad (Eq.\ 1)$$

$$Q\text{-}OR^{\bullet} + e \iff Q\text{-}OR^{2-} \qquad\qquad (Eq.\ 2)$$

During the electrochemical study of Q1, Q4, Q7, all hydroxylated quinones (Q-OH), the CV displayed an apparently simpler profile and only one couple is observed, which does not follow the typical two monoelectronic reversible charge transfer processes, occurring for the other quinones, as shown. The observed electrochemical behavior for those 5-hydroxyquinones is consistent with a reduction mechanism involving both electron transfer processes and coupled chemical reactions, where self-protonation processes occur. This occurs due to the high acidity of the hydroxyl function at the C-5 position in front of the first electrogenerated anion radical, as already shown for 2-hydroxyquinones [2,28] and specifically for juglone, in a different medium and working electrode [29]. It is interesting to note that the presence of self-protonation processes consumes quickly any stable radical species which could be generated at these energetic conditions [2] (Eq. 3). Despite the mild acid nature of the phenol in juglone, self-protonation was observed in higher concentration [29]. Due to that, the first wave is shifted to more positive potentials and is not evidenced on mercury electrodes.

$$3\ Q\text{-}OH + 2\ e\text{-} \rightarrow H_2Q\text{-}OH + 2\ Q\text{-}O^{-} \qquad\qquad (Eq.\ 3)$$
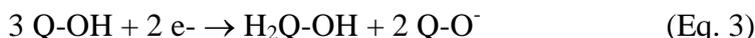
The observed wave (figure not shown) is related to the second reduction step and this signal is consistent with the reduction of the deprotonated quinone (Q-O$^-$) formed during the self-protonation sequence, leading to the formation of a radical dianion structure (Eq. 4). This type of intermediates can be characterized by employing coupled Electrochemical-Electron Spin Resonance (EC-ESR) experiments [30].

$$Q\text{–}O^{-} + e^{-} \rightleftharpoons Q\text{–}O^{\bullet =} \qquad\qquad (Eq.\ 4)$$
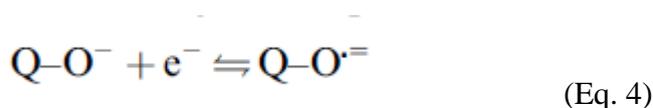
Table 1 lists the main electrochemical parameters in aprotic media.

Table 1. Cyclic voltammetric parameters of the quinones in aprotic medium (DMSO + 0.1 M TBAP), on Hg electrode vs. saturated calomel electrode, sweep rate 2.0 V s^{-1}

Compounds	EpIc (V)	EpIIc (V)
Q1	–	−1.004
Q2	−0.419	−0.736
Q3	−0.667	−1.271
Q4	–	−0.858
Q5	−0.371	−0.910
Q6	−0.481	−1.171
Q7	–	−0.857
Q8	−0.386	−0.959
Q9	−0.491	−1.160

It can be observed that the substitution on naphthoquinone moiety, as expected, modify the redox potential. The comparison should be made by dividing the quinones in two classes (Q-OR and Q-OH). Q-OH cannot be compared, except for the second wave, much more positive than the others. In the Q-OR class, the presence of the acetyl group (in Q2, Q5, Q8), facilitates the quinone reduction. The addition of Br at the quinone core in Q4 to Q9 leads to anodic shifts in the reduction potential, regardless the substitution position (Table 1).

3.2. Electrochemical studies in protic medium

Juglone (Q1) was chosen to represent the studied quinones. The cyclic voltammogram of Q1, performed using a GC electrode, in EtOH/acetate buffer solution (20%), pH 7.0, displays a reduction behavior, typical of well-behaved quinones in protic medium (mixed ethanolic aqueous buffered media) [31], represented by a bielectronic, diffusional, reversible pair of peaks (EpIc = –0.311 V, EpIa = –0.251 V), scan rate of 0.100 V s^{-1} (Figure 3A, Eq. 5), related to the full reduction of the quinone function. For QOR, similar mechanism occurs. In DPV performed on a GC electrode, the oxidation of Q1 was represented in the anodic sweep, by a peak Ia located at an EpIa of +1.00 V) (Figure 3B). For the nine naphthoquinones, CV and DPV were performed and the comparison between them is shown in figure 3. The acetyl derivatives Q2, Q5 and Q8 were not stable in this medium (they suffer hydrolysis) and their profiles were not shown. Table 2 lists the values of EpIc, using DPV.

$$Q\text{-}OH + 2e^- + 2 H^+ \Longleftrightarrow QH_2OH \qquad\qquad (Eq.\ 5)$$

It has been demonstrated that the redox properties of quinones are very strongly connected with their acid-base properties [31,32,33]. It is also well-known that biological activity in a live host is always a complex outcome not usually dominated by one parameter.

A
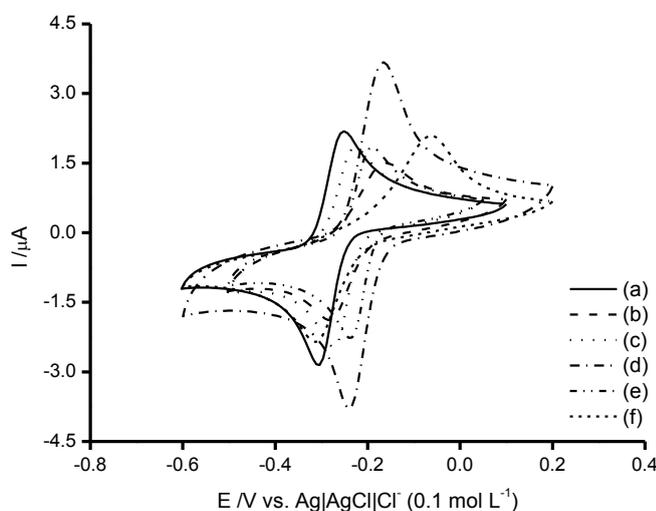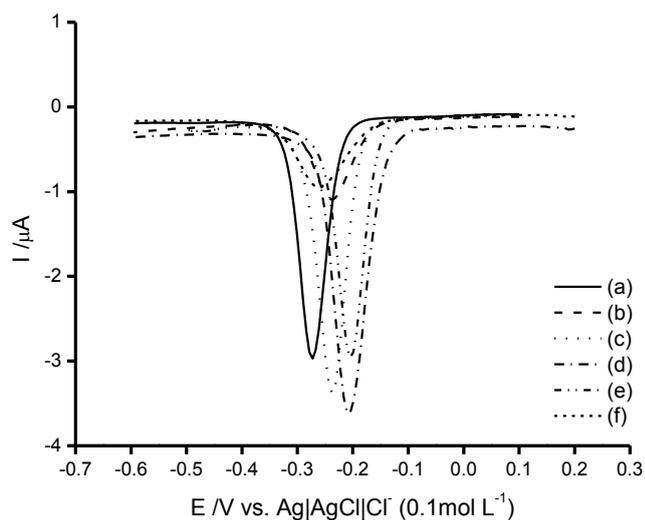
Figure 3. A) CV for the reduction of quinones Q1 (a), Q3 (b), Q4 (c), Q6 (d), Q7 (e) and Q9 (f), at concentration of 4.8×10^{-5} mol L^{-1} [phosphate buffer/ethanol (40 %, v/v), pH 7.0], on GCE, reference: Ag|AgCl|Cl$^-$ (0.1 mol L^{-1}), scan rate: 0.100 V s^{-1}. B) Differential pulse voltammograms (DPV) for the reduction of the quinones Q1 (a), Q3 (b), Q4 (c), Q6 (d), Q7 (e) and Q9 (f), at 4.8×10^{-5} mol L^{-1} [phosphate buffer/ethanol (40 %, v/v), pH 7.0], on GCE, reference: Ag|AgCl|Cl$^-$ (0.1 mol L^{-1}), scan rate: 0.005 V s^{-1}.

Several physico-chemical parameters have an important impact on pharmacokinetic and metabolic fate of the biologically active compounds in the body, and so, a good understanding of these properties, coupled with their measurement and prediction are crucial for the understanding of a biological mechanism of action. One of the most important is pKa, so it would be important to measure pKa values for juglone (Q1). For the measurement of pK_a values, it is necessary to expose the compound to an environment of changing pH and to monitor a particular property that changes as a function of the ionization state of the molecule, in this case, the reduction potential.

Table 2. Electrochemical parameters (EpIc), obtained from DPV, for analysed quinones, in phosphate buffer, pH 7, using GCE.

Compounds	EpIc (V)
Q1	-0.272
Q3	-0.239
Q4	-0.237
Q6	-0.204
Q7	-0.205
Q9	-0.213

The apparent dissociation constant (pKa) of Q1 was determined in aqueous buffer solutions + ethanol (4:1) mixtures, using DPV (Figure 4A). From this figure, it is noticeable that the reduction potentials for Q1 shift to more negative potentials, as the solution pH increases (Figure 4B). The pKa value was obtained in the intersection of the two straight lines, giving the value of 6.20, relative to the dissociation of the 5-OH group. In the literature, pKa values for the reduced juglone and for the semiquinone are reported [16].
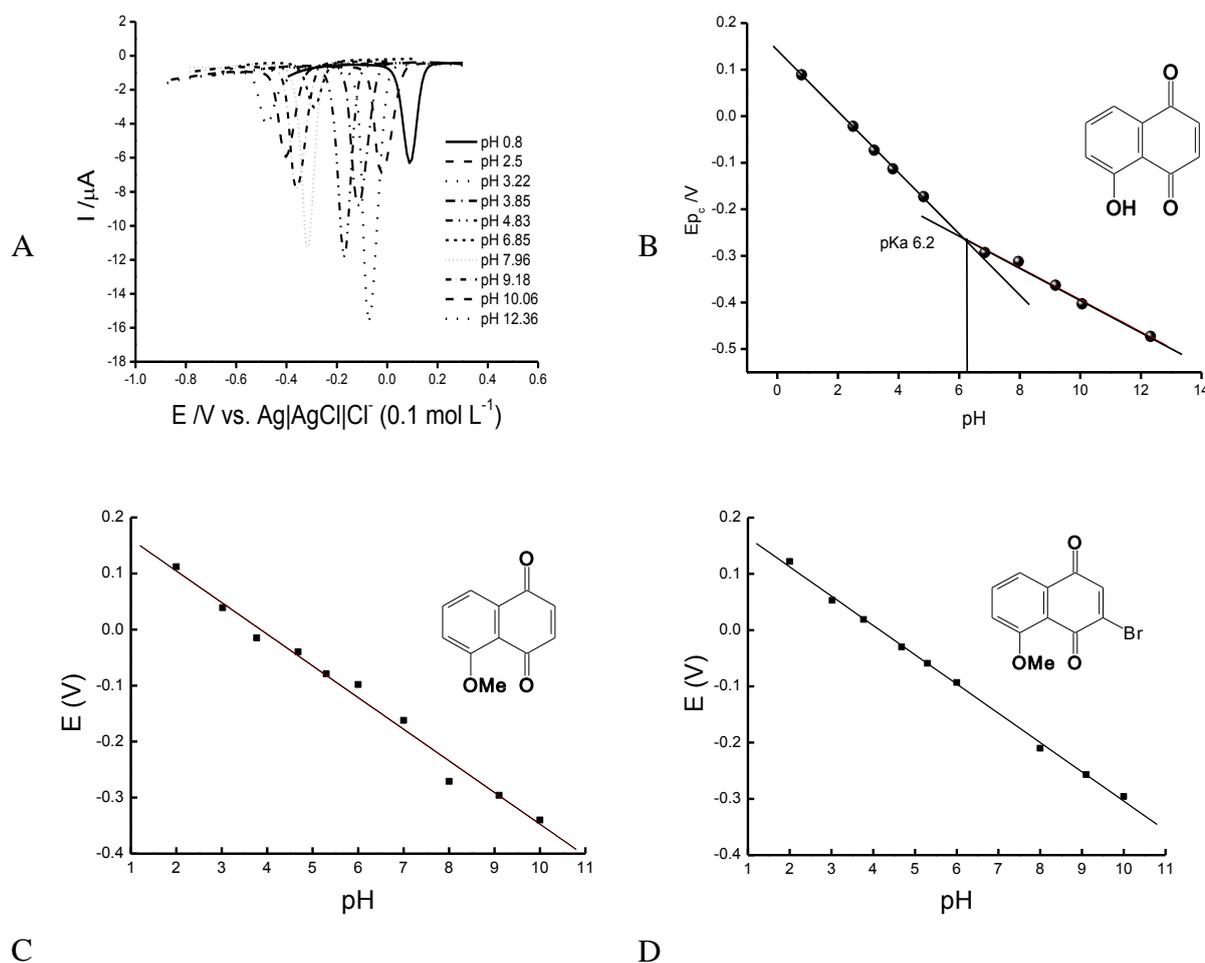
Figure 4. A) DPV for the reduction of Q1, $c_{Q1} = 1.0 \times 10^{-4}$ mol L^{-1}, in pH values from 0.8 a 12.36. Pulse Amplitude: 0.05 V, scan rate: 0.005 V s^{-1}, working electrode: GC, reference electrode: Ag|AgCl|Cl^{-} (0.1 mol L^{-1}), auxiliary electrode: platinum wire. B) Graph EpIc × pH. C) Graph EpIc × pH for Q2. D) Graph EpIc × pH for Q9.

The pH effects on the reduction behavior of Q2 and Q9 were also obtained (Figures 4C and D), with the same trend, as shown before. Simple manipulation of the Nernst equation shows that the observed redox potential for an m H^{+}, n e^{-} redox couple will change $-m/n$ (59 mV)/pH, at 25°C. So, under conditions where quinones undergo a 2 e^{-}, 2 H^{+} reduction, a plot of EpIc$_{app}$ vs. pH should give a slope of -59 mV/pH unit up to pH = pKa$_1$ for QH$_2$. That is indeed what occurs with Q2 (Figure 4B)

and Q9 (Figure 4C), with the first slope equal to -56.50 mV/pH unit, r = 0.9932 and -52.06 mV/pH unit, r = 0.9990, respectively.

3.3 Electron Spin Resonance

The free radicals derived from the quinones were prepared "in situ" by electrochemical reduction in DMSO, by applying a potential corresponding to the first monoelectronic wave (*E*pIc) for Q-OR and *E*pIIc (Table 1) for Q-O⁻ (the conjugated base of Q-OH), obtained from cyclic voltammograms and under the same experimental conditions (Figure 5).

Assignment of each hyperfine coupling constant (hfcc) value was performed by means of electronic structure calculations of the spin density and correlated with the experimental data. The ESR spectra of the different radical ions were simulated by the program WINEPR Simphonia using as starting point the experimental hyperfine pattern, changing different parameters up to finding the major coincidence between the simulated spectrum with the experimental one [34, 35].
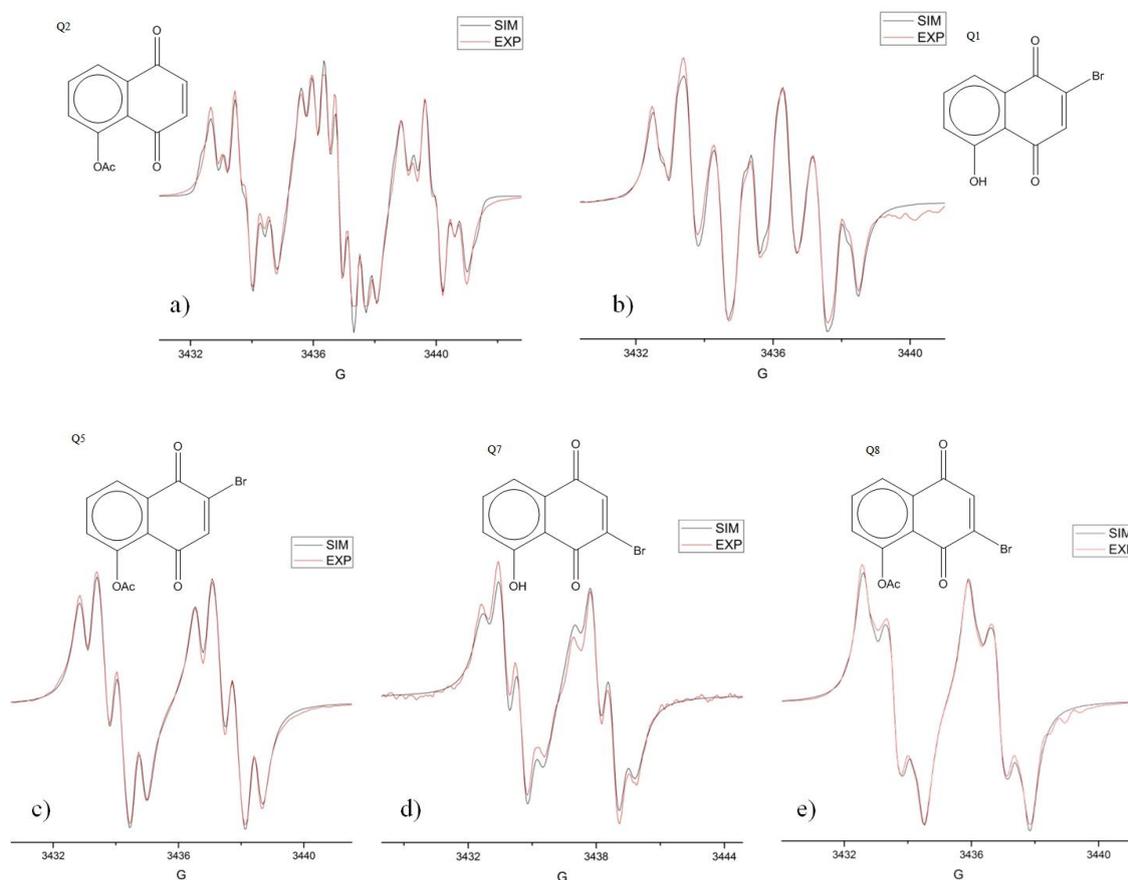
Figure 5. Experimental (red) and simulated (black) ESR spectra for semiquinone (Q-OR)$^{\bullet-}$ and (Q-O)$^{\bullet=}$ derivatives

For the successful use of the simulation programs the introduction of starting hfcc values is needed, in order to obtain a satisfactory correspondence with the experimental spectra. At the same

time many computational packages are able to provide hfcc values from quantum chemical calculations. Thus, between them the methods based on the density functional methods are known for its capacity of providing reasonable predictions for ESR calculations of hyperfine coupling constants [22-24]. In order to consider the line-widths effects that could be produced by the environment effects, it was used a software package developed by Rockenbauer [17] that includes several minimization methods to get the best agreement between the experimental and simulated spectra. Thus, the interpretation of the ESR spectrum by means of a simulation process has led to the determination of the hyperfine coupling constants for all the magnetic nuclei and therefore, the corresponding hyperfine pattern.

Comparing experimental values of hfcc with those predicted by the theoretical method (Table 3), a correlation among them was observed; the experimental value is finely reproduced by these methods, and the electronic structure studies have been an essential tool to aid the interpretation of ESR data; thus, a description of physicochemical parameter such as the hyperfine coupling constant as well as a "tridimensional perspective" by mapping the spin density of unpaired electron over the molecule were obtained (Figure 6). A good agreement between the experimental and simulated ESR spectra (Figure 5) ensures the correct elucidation of the hyperfine pattern for this radical, that can be described in terms of five doublets corresponding to the hydrogens H-2, -3, -6, -7 and H-8, respectively.

Table 3. Experimental and theoretical hyperfine coupling constants for Q1-Q9*[+]

Compounds	aH(2)	aH(3)	aH(8)	aH(6)	aH(7)
Q1	2.82(2.38)	3.60(3.88)	1.05(0.91)	1.58(1.54)	0.60(0.62)
Q2	2.89(2.80)	3.29 (3.20)	0.76(0.75)	0.81 (0.80)	0.29(0.33)
Q3	2.35(2.86)	3.87(4.2)	0.75(0.66)	1.39(1.14)	0.69(0.54)
Q4	Br	2.88(2.8)	0.88(0.8)	1.04(0.82)	0.66(0.78)
Q5	Br	3.68(3.7)	0.75(0.65)	0.63(0.65)	0.56(0.65)
Q6	Br	4.79(4.13)	0.97(0.65)	1.40(0.97)	0.38(0.45)
Q7	4.28(4.29)	Br	0.81(0.91)	0.81(0.91)	0.81(0.89)
Q8	3.31(3.31)	Br	0.83(0.7)	0.57(0.78)	<
Q9	3.05(3.44)	Br	0.54(0.59)	1.03(0.96)	0.81(0.52)

* Theoretical hyperfine coupling constants in parenthesis. Model used: UB3LYP/6-31G+(CPCM=DMSO), [+] Coupling constants in Gauss units.

Starting from spin density map of unpaired electron (Figure 6), one may observe a larger delocalization mainly over the quinone moiety; this is extended throughout the aromatic moiety. The high delocalization was clearly evidenced by the hyperfine coupling of H-7 with the larger coupling constant, besides the couplings at the H-3 (close to the quinone moiety) and H-6 (far from quinone) positions.

The theoretical estimations give indicia in respect to spin distribution of unpaired electron. Herein, an accurate description of the hyperfine system with a large concordance between the theoretical values with the experimental ones was obtained. All the theoretical methodologies, herein used, are consistent with the experimental pattern proposed below:

The experimental spectra detected for the corresponding semiquinones of Q2 (Figure 5) are characterized by the presence of five hfcc values, each corresponding to one non-equivalent hydrogen nuclei that interacts with the unpaired electronic spin (Table 3). The highest coupling constants correspond to the hydrogen in position 3 and in position 2, suggesting that the unpaired electron is more located at the quinone moiety. It is interesting to note that when there is no Br in the naphthoquinone ring, the two hydrogens (H-2 and H-3) are detected with similar magnitudes, which are expressed in the ESR spectrum like a triplet of large size as consequence of the superimposition of lines (Figure 5A).
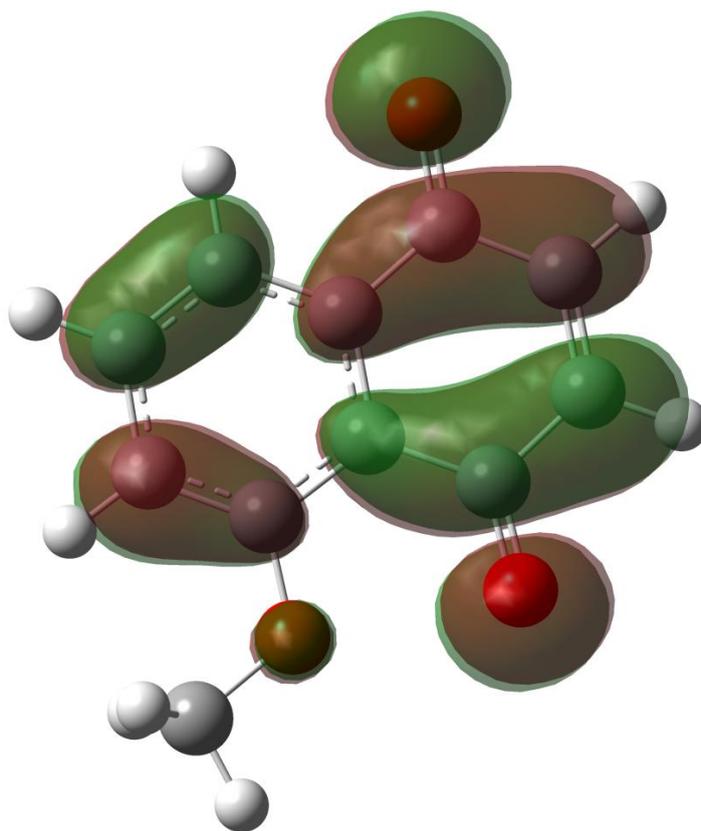
Figure 6. Spin density of the unpaired electron on the semiquinone derivative Q3$^{\bullet}$.

The ESR spectra (Figure 5) of the radicals derived from Q4, Q5 and Q6 were well resolved. The unpaired electron interacts with each non-equivalent hydrogens: H-6, H-8, H-7, H-3. It seems that it does not modify the spin density of the radical in presence of the Br nuclei. However, the presence of Br on the naphthoquinone ring generates an ESR spectrum different from those without Br, showing a doublet with a large coupling constant that defines the shape of the last ones. The hyperfine splitting

on the ESR spectra of the monoelectronic radical for Q7, Q8 and Q9 (Figure 4d) is explained by the assignment of the constants given in Table 3. The unpaired electron interacts with the hydrogens: H-6, H-8, H-7 and H-2, producing four doublets. H-2 has a higher spin density (especially in Q-O$^-$), then, confirming that the unpaired electron is located on the naphthoquinone moiety, for the concentration values used in this work fragment.

In summary, all the naphthoquinones were successfully described. The hyperfine pattern proposed for this family is in complete agreement with the theoretical and experimental data, which validates the theoretical models used and the interpretation of the hyperfine spectra.

4. CONCLUSIONS

The electrochemical behavior for all quinone derivatives in aprotic and protic media were in agreement with classical behaviour. The presence of Br in the quinone moiety facilitates the reduction in both media, and the acetyl group present in Q2, Q5 and Q8 exerts the withdrawing effect in aprotic medium. Theoretical and experimental values were similar. The hyperfine structure of the radicals studied and the magnitude of the hyperfine couplings of each radical was evaluated through the simulation of the experimental spectra which confirmed the proposed patterns.

References

1. E. A. Hillard, F. C. de Abreu, D. C. M. Ferreira, G. Jaouen, M. O. F. Goulart, C. Amatore, *Chem. Commun.*, (2008) 2612-2628.
2. C. Frontana, I. Gonzalez, *J. Electroanal. Chem.*, 603 (2007) 155–165.
3. G. Roura-Pérez, B. Quiróz, M. Aguilar-Martínez, C. Frontana, A. Solano, I. González, J. A. Bautista-Martínez, J. Jiménez-Barbero, G. Cuevas, *J. Org. Chem.*, 72 (2007) 1883-1894.
4. D. M. Hernandez, M. A. B. F. de Moura, D. P. Valencia, F. J. Gonzalez, I. Gonzalez, F. C. de Abreu, E. N. da Silva Junior, V. F. Ferreira, A. V. Pinto, M. O. F. Goulart, C. Frontana, *Org. Biomol. Chem.*, 6 (2008) 3414-3420.
5. F. C. de Abreu, P.A.L. Ferraz, M.O.F. Goulart, *J. Braz. Chem. Soc.*, 13 (2002) 19-35.
6. C.-Y. Li, J. Jenq, *Electrochim. Acta*, 36 (1991) 269-276.
7. P. W. Crawford, J. Gross, K. Lawson, C. C. Cheng, Q. Dong, D. F. Liu, Y. L. Luo, B. G. Szczepankiewicz, C. H. Heathcock, *J. Electrochem. Soc.*, 144 (1997) 3710-3715.
8. D. Jezziorek, T. Ossowski, A. Liwo, D. Dyl, M. Nowacka, W. Woznicki, *J. Chem. Soc.*, *Perkin Trans.*, 2 (1997) 229-236.
9. H. Weiss, T. Friedrich, G. Hofhaus, D. Preis, *Eur. J. Biochem.*, 197 (1991) 563-576.
10. A. Ashnagar, J. M. Bruce, P. L. Dutton, R. C. Prince, *Biochim. Biophys. Acta*, 801 (1984) 351-359.

11. P. W. Crawford, E. Carlos, J. C. Ellegood, C. C. Cheng, Q. Dong, D. F. Liu, Y. L. Luo, *Electrochim. Acta*, 41 (1996) 2399-2403.
12. P. Babula, V. Adam, L. Havel, R. Kizek, *Curr. Pharmaceutical Anal.*, 5 (2009) 47-68.
13. R. C. Montenegro, A. J. Araújo, M. T. Molina, J. D. B. M. Filho, D. D. Rocha, E. Lopéz-Montero, M. O. F. Goulart, E. S. Bento, A. P. N. N. Alves, C. Pessoa, M. O. de Moraes, L. V. Costa-Lotufo, *Chem-Biol. Inter.*, 184 (2010) 439-448.
14. K. A. L. Ribeiro, C. M. de Carvalho, M. T. Molina, E. P. Lima, E. López-Montero, J. R. M. Reys, M. B. F. de Oliveira, A. V. Pinto, A. E. G. Santana, M. O. F. Goulart, *Acta Tropica,* 111 (2009) 44-50.
15. L. S. Hernandez-Munoz, M. Gomez, F. J. Gonzalez, I. Gonzalez, C. Frontana, *Org. Biomol. Chem.*, 7 (2009) 1896-1903.
16. Z. Anusevicius, J. Sarlauskas, N. Cenas, *Arch. Biochem. Biophys.*, 404 (2002) 254–262
17. A. Rockenbauer, L. Korecz, *Appl. Magn. Res.*, 10 (1996) 29-43.
18. Spartan' 04. Wavefunction Inc, 18401 Von Karman Avenue, Suite 370, Irvine, California 92612, USA.
19. P. C. Spartan '04 User's Guide, Wavefunction Inc, California.
20. M. J. S. Dewar, E. G. Zoebisch, E. F. Healy, J. J. P. Stewart, *J. Amer. Chem. Soc.*, 107 (1985) 3902-3909.
21. G. W. T. M. J. Frisch, H. B. Schlegel, G. E. Scuseria, M. A. Robb, J. R. Cheeseman, J. A. Montgomery, Jr., T. Vreven, K. N. Kudin, J. C. Burant, J. M. Millam, S. S. Iyengar, J. Tomasi, V. Barone, B. Mennucci, M. Cossi, G. Scalmani, N. Rega, G. A. Petersson, H. Nakatsuji, M. Hada, M. Ehara, K. Toyota, R. Fukuda, J. Hasegawa, M. Ishida, T. Nakajima, Y. Honda, O. Kitao, H. Nakai, M. Klene, X. Li, J. E. Knox, H. P. Hratchian, J. B. Cross, V. Bakken, C. Adamo, J. Jaramillo, R. Gomperts, R. E. Stratmann, O. Yazyev, A. J. Austin, R. Cammi, C. Pomelli, J. W. Ochterski, P. Y. Ayala, K. Morokuma, G. A. Voth, P. Salvador, J. J. Dannenberg, V. G. Zakrzewski, S. Dapprich, A. D. Daniels, M. C. Strain, O. Farkas, D. K. Malick, A. D. Rabuck, K. Raghavachari, J. B. Foresman, J. V. Ortiz, Q. Cui, A. G. Baboul, S. Clifford, J. Cioslowski, B. B. Stefanov, G. Liu, A. Liashenko, P. Piskorz, I. Komaromi, R. L. Martin, D. J. Fox, T. Keith, M. A. Al-Laham, C. Y. Peng, A. Nanayakkara, M. Challacombe, P. M. W. Gill, B. Johnson, W. Chen, M. W. Wong, C. Gonzalez, J. A. Pople, *Gaussian, Inc.*, Wallingford CT, 2004. Gaussian.Com.
22. M. D'Amore, R. Improta, V. Barone, *J. Phys. Chem.*, A 107 (2003) 6264-6269.
23. A. D. Becke, *Phys. Rev.*, A 38 (1988) 3098-3100.
24. C. T. Lee, W. T. Yang, R. G. Parr, *Phys. Rev.*, B 37 (1988) 785-789.
25. B. Aguilera-Venegas, C. Olea-Azar, E. Norambuena, V. J. Arán, F. Mendizábal, M. Lapier, J. D. Maya, U. Kemmerling, R. López-Muñoz, *Spectrochim. Acta Part A: Molecular and Biomolecular Spectroscopy*, 78 (2011) 1004-1012.
26. V. Barone, M. Cossi, *J. Phys. Chem., A* 102 (1998) 1995-2001.
27. M. Cossi, V. Barone, R. Cammi, J. Tomasi, *Chem. Phys. Letters*, 255 (1996) 327-335.
28. P. A. L. Ferraz, F. C. Abreu, A. V. Pinto, V. Glezer, J. Tonholo, M. O. F. Goulart, *J. Electroanal. Chem.*, 507 (2001) 275-286.
29. L. S. Hernandez-Munoz, M. Gomez, F. J. Gonzalez, I. Gonzalez, C. Frontana, *Org. Biomol. Chem.*, 7 (2009) 1896-1903.
30. C. Frontana, B. A. Frontana-Uribe, I. Gonzalez, *J. Electroanal. Chem.*, 573 (2004) 307.
31. F. C. Abreu, M. O. F. Goulart, A. M. O. Brett, *Electroanalysis*, 14 (2002) 29-34.
32. T. Ossowski, M. O. F. Goulart, F. C. Abreu, A. E. G. Sant'Ana, P. R. B. Miranda, C. O. Costa, A. Liwo, P. Falkowski, D. Zarzeczanska, *J. Braz. Chem. Soc.*, 19 (2008) 175-183.
33. S. Klod, L. Dunsch, *Magn. Reson. Chem. 49* (2011) 725–729
34. C. Rigol, C. Olea-Azar, F. Mendizábal, L. Otero, D. Gambino, M. González, H. Cerecetto, *Spectrochim. Acta Part A: Mol. Biomol. Spectroscopy*, 61 (2005) 2933-2938.

35. J. Rodríguez, C. Olea-Azar, G. Barriga, C. Folch, A. Gerpe, H. Cerecetto, M. González, *Spectrochim. Acta Part A: Mol. Biomol. Spectroscopy*, 70 (2008) 557-563.